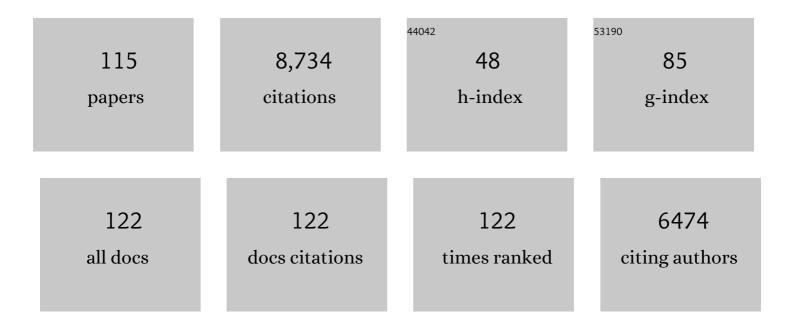
## **Cathy Clerbaux**

List of Publications by Year in descending order

Source: https://exaly.com/author-pdf/7369595/publications.pdf Version: 2024-02-01



#	Article	IF	CITATIONS
1	Monitoring of atmospheric composition using the thermal infrared IASI/MetOp sounder. Atmospheric Chemistry and Physics, 2009, 9, 6041-6054.	1.9	694
2	The MACC reanalysis: an 8 yr data set of atmospheric composition. Atmospheric Chemistry and Physics, 2013, 13, 4073-4109.	1.9	424
3	Global ammonia distribution derived from infrared satellite observations. Nature Geoscience, 2009, 2, 479-483.	5.4	400
4	Hyperspectral Earth Observation from IASI: Five Years of Accomplishments. Bulletin of the American Meteorological Society, 2012, 93, 347-370.	1.7	357
5	Towards a climate-dependent paradigm of ammonia emission and deposition. Philosophical Transactions of the Royal Society B: Biological Sciences, 2013, 368, 20130166.	1.8	328
6	Industrial and agricultural ammonia point sources exposed. Nature, 2018, 564, 99-103.	13.7	312
7	Atmospheric ammonia and particulate inorganic nitrogen over the United States. Atmospheric Chemistry and Physics, 2012, 12, 10295-10312.	1.9	240
8	Tropospheric Ozone Assessment Report: Present-day distribution and trends of tropospheric ozone relevant to climate and global atmospheric chemistry model evaluation. Elementa, 2018, 6, .	1.1	240
9	Carbon monoxide distributions from the IASI/METOP mission: evaluation with other space-borne remote sensors. Atmospheric Chemistry and Physics, 2009, 9, 8317-8330.	1.9	208
10	Global distributions, time series and error characterization of atmospheric ammonia (NH <sub>3</sub> ) from IASI satellite observations. Atmospheric Chemistry and Physics, 2014, 14, 2905-2922.	1.9	195
11	Satellite evidence for a large source of formic acid from boreal and tropical forests. Nature Geoscience, 2012, 5, 26-30.	5.4	171
12	IASI measurements of reactive trace species in biomass burning plumes. Atmospheric Chemistry and Physics, 2009, 9, 5655-5667.	1.9	165
13	FORLI radiative transfer and retrieval code for IASI. Journal of Quantitative Spectroscopy and Radiative Transfer, 2012, 113, 1391-1408.	1.1	162
14	Retrieval of sulphur dioxide from the infrared atmospheric sounding interferometer (IASI). Atmospheric Measurement Techniques, 2012, 5, 581-594.	1.2	150
15	Tracking the emission and transport of pollution from wildfires using the IASI CO retrievals: analysis of the summer 2007 Greek fires. Atmospheric Chemistry and Physics, 2009, 9, 4897-4913.	1.9	147
16	First space-based derivation of the global atmospheric methanol emission fluxes. Atmospheric Chemistry and Physics, 2011, 11, 4873-4898.	1.9	122
17	ACE-FTS observation of a young biomass burning plume: first reported measurements of C <sub>2</sub> H <sub>4</sub> , C <sub>3</sub> H <sub>6</sub> O, H <sub>2</sub> CO and PAN by infrared occultation from space.	1.9	119
18	Atmospheric Chemistry and Physics, 2007, 7, 5407-5446. Satellite monitoring of ammonia: A case study of the San Joaquin Valley. Journal of Geophysical Research, 2010, 115	3.3	118

#	Article	IF	CITATIONS
19	Version 2 of the IASI NH <sub>3</sub> neural network retrieval algorithm: near-real-time and reanalysed datasets. Atmospheric Measurement Techniques, 2017, 10, 4905-4914.	1.2	118
20	Towards IASI-New Generation (IASI-NG): impact of improved spectral resolution and radiometric noise on the retrieval of thermodynamic, chemistry and climate variables. Atmospheric Measurement Techniques, 2014, 7, 4367-4385.	1.2	110
21	Retrieval and characterization of ozone vertical profiles from a thermal infrared nadir sounder. Journal of Geophysical Research, 2005, 110, .	3.3	108
22	A Regularized Neural Net Approach for Retrieval of Atmospheric and Surface Temperatures with the IASI Instrument. Journal of Applied Meteorology and Climatology, 2002, 41, 144-159.	1.7	107
23	Trace gas measurements from infrared satellite for chemistry and climate applications. Atmospheric Chemistry and Physics, 2003, 3, 1495-1508.	1.9	107
24	Surface-to-space atmospheric waves from Hunga Tonga–Hunga Ha'apai eruption. Nature, 2022, 609, 741-746.	13.7	107
25	A unified approach to infrared aerosol remote sensing and type specification. Atmospheric Chemistry and Physics, 2013, 13, 2195-2221.	1.9	105
26	Validation of three different scientific ozone products retrieved from IASI spectra using ozonesondes. Atmospheric Measurement Techniques, 2012, 5, 611-630.	1.2	102
27	Operational trace gas retrieval algorithm for the Infrared Atmospheric Sounding Interferometer. Journal of Geophysical Research, 2004, 109, n/a-n/a.	3.3	99
28	Analysis of ozone and nitric acid in spring and summer Arctic pollution using aircraft, ground-based, satellite observations and MOZART-4 model: source attribution and partitioning. Atmospheric Chemistry and Physics, 2012, 12, 237-259.	1.9	96
29	A flexible and robust neural network IASIâ€NH <sub>3</sub> retrieval algorithm. Journal of Geophysical Research D: Atmospheres, 2016, 121, 6581-6599.	1.2	96
30	The influence of boreal biomass burning emissions on the distribution of tropospheric ozone over North America and the North Atlantic during 2010. Atmospheric Chemistry and Physics, 2012, 12, 2077-2098.	1.9	90
31	Towards validation of ammonia (NH <sub>3</sub> ) measurements from the IASI satellite. Atmospheric Measurement Techniques, 2015, 8, 1575-1591.	1.2	90
32	NH <sub>3</sub> emissions from large point sources derived from CrIS and IASI satellite observations. Atmospheric Chemistry and Physics, 2019, 19, 12261-12293.	1.9	89
33	Thermal infrared nadir observations of 24 atmospheric gases. Geophysical Research Letters, 2011, 38, n/a-n/a.	1.5	88
34	Ten years of CO emissions as seen from Measurements of Pollution in the Troposphere (MOPITT). Journal of Geophysical Research, 2011, 116, .	3.3	87
35	Retrieving radius, concentration, optical depth, and mass of different types of aerosols from high-resolution infrared nadir spectra. Applied Optics, 2010, 49, 3713.	2.1	80
36	Ammonia emissions in tropical biomass burning regions: Comparison between satellite-derived emissions and bottom-up fire inventories. Atmospheric Environment, 2015, 121, 42-54.	1.9	78

#	Article	IF	CITATIONS
37	Exceptional emissions of NH <sub>3</sub> and HCOOH in the 2010 Russian wildfires. Atmospheric Chemistry and Physics, 2013, 13, 4171-4181.	1.9	76
38	Summertime tropospheric ozone assessment over the Mediterranean region using the thermal infrared IASI/MetOp sounder and the WRF-Chem model. Atmospheric Chemistry and Physics, 2014, 14, 10119-10131.	1.9	73
39	Global distributions of methanol and formic acid retrieved for the first time from the IASI/MetOp thermal infrared sounder. Atmospheric Chemistry and Physics, 2011, 11, 857-872.	1.9	71
40	Ubiquitous atmospheric production of organic acids mediated by cloud droplets. Nature, 2021, 593, 233-237.	13.7	71
41	Land surface skin temperatures from a combined analysis of microwave and infrared satellite observations for an all-weather evaluation of the differences between air and skin temperatures. Journal of Geophysical Research, 2003, 108, .	3.3	70
42	Carbon monoxide pollution from cities and urban areas observed by the Terra/MOPITT mission. Geophysical Research Letters, 2008, 35, .	1.5	68
43	Worldwide spatiotemporal atmospheric ammonia (NH <sub>3</sub> ) columns variability revealed by satellite. Geophysical Research Letters, 2015, 42, 8660-8668.	1.5	66
44	IASI carbon monoxide validation over the Arctic during POLARCAT spring and summer campaigns. Atmospheric Chemistry and Physics, 2010, 10, 10655-10678.	1.9	65
45	Global, regional and national trends of atmospheric ammonia derived from a decadal (2008–2018) satellite record. Environmental Research Letters, 2021, 16, 055017.	2.2	65
46	The unintended consequence of SO <sub>2</sub> and NO <sub>2</sub> regulations over China: increase of ammonia levels and impact on PM <sub>2.5</sub> concentrations. Atmospheric Chemistry and Physics, 2019, 19, 6701-6716.	1.9	63
47	Evaluating 4 years of atmospheric ammonia (NH <sub>3</sub> ) over Europe using IASI satellite observations and LOTOSâ€EUROS model results. Journal of Geophysical Research D: Atmospheres, 2014, 119, 9549-9566.	1.2	61
48	Record high levels of atmospheric ammonia over India: Spatial and temporal analyses. Science of the Total Environment, 2020, 740, 139986.	3.9	61
49	An evaluation of IASI-NH <sub>3</sub> with ground-based Fourier transform infrared spectroscopy measurements. Atmospheric Chemistry and Physics, 2016, 16, 10351-10368.	1.9	56
50	An examination of the long-term CO records from MOPITT and IASI: comparison of retrieval methodology. Atmospheric Measurement Techniques, 2015, 8, 4313-4328.	1.2	50
51	Substantial Underestimation of Post-Harvest Burning Emissions in the North China Plain Revealed by Multi-Species Space Observations. Scientific Reports, 2016, 6, 32307.	1.6	49
52	Interannual variability of ammonia concentrations over the United States: sources and implications. Atmospheric Chemistry and Physics, 2016, 16, 12305-12328.	1.9	48
53	Validation of the IASI FORLI/EUMETSAT ozone products using satellite (GOME-2), ground-based (Brewer–Dobson, SAOZ, FTIR) and ozonesonde measurements. Atmospheric Measurement Techniques, 2018, 11, 5125-5152.	1.2	47
54	Validation of IASI FORLI carbon monoxide retrievals using FTIR data from NDACC. Atmospheric Measurement Techniques, 2012, 5, 2751-2761.	1.2	45

#	Article	IF	CITATIONS
55	First space-based observations of formic acid (HCOOH): Atmospheric Chemistry Experiment austral spring 2004 and 2005 Southern Hemisphere tropical-mid-latitude upper tropospheric measurements. Geophysical Research Letters, 2006, 33, .	1.5	42
56	On the capability of IASI measurements to inform about CO surface emissions. Atmospheric Chemistry and Physics, 2009, 9, 8735-8743.	1.9	42
57	Validation of the MetOp-A total ozone data from GOME-2 and IASI using reference ground-based measurements at the Iberian Peninsula. Remote Sensing of Environment, 2011, 115, 1380-1386.	4.6	42
58	IASI observations of sulfur dioxide (SO <sub>2</sub> ) in the boundary layer of Norilsk. Journal of Geophysical Research D: Atmospheres, 2014, 119, 4253-4263.	1.2	42
59	Tropospheric ozone and nitrogen dioxide measurements in urban and rural regions as seen by IASI and GOMEâ€2. Journal of Geophysical Research D: Atmospheres, 2013, 118, 10,555.	1.2	41
60	Doubling of annual ammonia emissions from the peat fires in Indonesia during the 2015 El Niño. Geophysical Research Letters, 2016, 43, 11,007.	1.5	41
61	Antarctic Ozone Enhancement During the 2019 Sudden Stratospheric Warming Event. Geophysical Research Letters, 2020, 47, e2020GL087810.	1.5	40
62	An inversion algorithm using neural networks to retrieve atmospheric CO total columns from high-resolution nadir radiances. Journal of Geophysical Research, 1999, 104, 23841-23854.	3.3	39
63	Tracking down global NH <sub>3</sub> point sources with wind-adjusted superresolution. Atmospheric Measurement Techniques, 2019, 12, 5457-5473.	1.2	39
64	A General Framework for Global Retrievals of Trace Gases From IASI: Application to Methanol, Formic Acid, and PAN. Journal of Geophysical Research D: Atmospheres, 2018, 123, 13,963.	1.2	38
65	Unaccounted variability in NH 3 agricultural sources detected by IASI contributing to European spring haze episode. Geophysical Research Letters, 2016, 43, 5475-5482.	1.5	37
66	Retrieval of near-surface sulfur dioxide (SO <sub>2</sub> ) concentrations at a global scale using IASI satellite observations. Atmospheric Measurement Techniques, 2016, 9, 721-740.	1.2	36
67	New Directions: Infrared remote sensing of the troposphere from satellite: Less, but better. Atmospheric Environment, 2013, 72, 24-26.	1.9	34
68	Intercontinental transport of anthropogenic sulfur dioxide and other pollutants: An infrared remote sensing case study. Geophysical Research Letters, 2011, 38, n/a-n/a.	1.5	32
69	O 3 variability in the troposphere as observed by IASI over 2008–2016: Contribution of atmospheric chemistry and dynamics. Journal of Geophysical Research D: Atmospheres, 2017, 122, 2429-2451.	1.2	32
70	A Decadal Data Set of Global Atmospheric Dust Retrieved From IASI Satellite Measurements. Journal of Geophysical Research D: Atmospheres, 2019, 124, 1618-1647.	1.2	32
71	Ammonia and PM2.5 Air Pollution in Paris during the 2020 COVID Lockdown. Atmosphere, 2021, 12, 160.	1.0	32
72	Monitoring emissions from the 2015 Indonesian fires using CO satellite data. Philosophical Transactions of the Royal Society B: Biological Sciences, 2018, 373, 20170307.	1.8	31

#	Article	IF	CITATIONS
73	Analysis of IASI tropospheric O <sub>3</sub> data over the Arctic during POLARCAT campaigns in 2008. Atmospheric Chemistry and Physics, 2012, 12, 7371-7389.	1.9	29
74	Validation of IASI Satellite Ammonia Observations at the Pixel Scale Using In Situ Vertical Profiles. Journal of Geophysical Research D: Atmospheres, 2021, 126, e2020JD033475.	1.2	28
75	Antarctic ozone hole as observed by IASI/MetOp for 2008–2010. Atmospheric Measurement Techniques, 2012, 5, 123-139.	1.2	27
76	Ozone variability in the troposphere and the stratosphere from the first 6 years of IASI observations (2008–2013). Atmospheric Chemistry and Physics, 2016, 16, 5721-5743.	1.9	25
77	Unprecedented Atmospheric Ammonia Concentrations Detected in the High Arctic From the 2017 Canadian Wildfires. Journal of Geophysical Research D: Atmospheres, 2019, 124, 8178-8202.	1.2	25
78	Spectroscopic measurements of halocarbons and hydrohalocarbons by satellite-borne remote sensors. Journal of Geophysical Research, 2003, 108, .	3.3	24
79	Atmospheric ammonia (NH3) emanations from Lake Natron's saline mudflats. Scientific Reports, 2019, 9, 4441.	1.6	24
80	Atmospheric ammonia variability and link with particulate matter formation: a case study over the Paris area. Atmospheric Chemistry and Physics, 2020, 20, 577-596.	1.9	24
81	Assimilation of IASI satellite CO fields into a global chemistry transport model for validation against aircraft measurements. Atmospheric Chemistry and Physics, 2012, 12, 4493-4512.	1.9	23
82	IASI's sensitivity to near-surface carbon monoxide (CO): Theoretical analyses and retrievals on test cases. Journal of Quantitative Spectroscopy and Radiative Transfer, 2017, 189, 428-440.	1.1	23
83	Topâ€Down CO Emissions Based On IASI Observations and Hemispheric Constraints on OH Levels. Geophysical Research Letters, 2018, 45, 1621-1629.	1.5	23
84	Tracking pollutants from space: Eight years of IASI satellite observation. Comptes Rendus - Geoscience, 2015, 347, 134-144.	0.4	21
85	Spaceborne Measurements of Formic and Acetic Acids: A Global View of the Regional Sources. Geophysical Research Letters, 2020, 47, e2019GL086239.	1.5	21
86	Extending the satellite data record of tropospheric ozone profiles from Aura-TES to MetOp-IASI: characterisation of optimal estimation retrievals. Atmospheric Measurement Techniques, 2014, 7, 4223-4236.	1.2	19
87	Acetone Atmospheric Distribution Retrieved From Space. Geophysical Research Letters, 2019, 46, 2884-2893.	1.5	18
88	Ten-Year Assessment of IASI Radiance and Temperature. Remote Sensing, 2020, 12, 2393.	1.8	18
89	Monthly Patterns of Ammonia Over the Contiguous United States at 2â€km Resolution. Geophysical Research Letters, 2021, 48, e2020GL090579.	1.5	16
90	First characterization and validation of FORLI-HNO <sub>3</sub> vertical profiles retrieved from IASI/Metop. Atmospheric Measurement Techniques, 2016, 9, 4783-4801.	1.2	15

#	Article	IF	CITATIONS
91	Decrease in tropospheric O <sub>3</sub> levels in the Northern Hemisphere observed by IASI. Atmospheric Chemistry and Physics, 2018, 18, 6867-6885.	1.9	14
92	Investigating the Long-Range Transport of Aerosol Plumes Following the Amazon Fires (August 2019): A Multi-Instrumental Approach from Ground-Based and Satellite Observations. Remote Sensing, 2020, 12, 3846.	1.8	14
93	HCOOH distributions from IASI for 2008–2014: comparison with ground-based FTIR measurements and a global chemistry-transport model. Atmospheric Chemistry and Physics, 2016, 16, 8963-8981.	1.9	13
94	Atmospheric Impacts of COVID-19 on NOx and VOC Levels over China Based on TROPOMI and IASI Satellite Data and Modeling. Atmosphere, 2021, 12, 946.	1.0	13
95	Present and future land surface and wet bulb temperatures in the Arabian Peninsula. Environmental Research Letters, 2022, 17, 044029.	2.2	13
96	IASI-derived NH <sub>3</sub> enhancement ratios relative to CO for the tropical biomass burning regions. Atmospheric Chemistry and Physics, 2017, 17, 12239-12252.	1.9	12
97	APIFLAME v2.0 biomass burning emissions model: impact of refined input parameters on atmospheric concentration in Portugal in summer 2016. Geoscientific Model Development, 2020, 13, 2981-3009.	1.3	12
98	The Diel Cycle of NH <sub>3</sub> Observed From the FYâ€4A Geostationary Interferometric Infrared Sounder (GIIRS). Geophysical Research Letters, 2021, 48, e2021GL093010.	1.5	11
99	Do alternative inventories converge on the spatiotemporal representation of spring ammonia emissions in France?. Atmospheric Chemistry and Physics, 2020, 20, 13481-13495.	1.9	11
100	Artificial Neural Networks to Retrieve Land and Sea Skin Temperature from IASI. Remote Sensing, 2020, 12, 2777.	1.8	10
101	Bottleneck Channels Algorithm for Satellite Data Dimension Reduction: A Case Study for IASI. IEEE Transactions on Geoscience and Remote Sensing, 2018, 56, 6069-6081.	2.7	9
102	Is the recovery of stratospheric O <sub>3</sub> speeding up in the Southern Hemisphere? An evaluation from the first IASI decadal record (2008–2017). Atmospheric Chemistry and Physics, 2019, 19, 14031-14056.	1.9	9
103	Identification of Short and Longâ€Lived Atmospheric Trace Gases From IASI Space Observations. Geophysical Research Letters, 2021, 48, e2020GL091742.	1.5	9
104	Trends in spectrally resolved outgoing longwave radiation from 10 years of satellite measurements. Npj Climate and Atmospheric Science, 2021, 4, .	2.6	8
105	First retrievals of peroxyacetyl nitrate (PAN) from ground-based FTIR solar spectra recorded at remote sites, comparison with model and satellite data. Elementa, 2021, 9, .	1.1	7
106	Multiscale observations of NH <sub>3</sub> around Toronto, Canada. Atmospheric Measurement Techniques, 2021, 14, 905-921.	1.2	7
107	Spectrally Resolved Fluxes from IASI Data: Retrieval Algorithm for Clear-Sky Measurements. Journal of Climate, 2020, 33, 6971-6988.	1.2	7
108	Determination of enhancement ratios of HCOOH relative to CO in biomass burning plumes by the Infrared Atmospheric Sounding Interferometer (IASI). Atmospheric Chemistry and Physics, 2017, 17, 11089-11105.	1.9	6

#	Article	IF	CITATIONS
109	Model and Satellite Analysis of Transport of Asian Anthropogenic Pollution to the Arctic: Siberian and Pacific Pathways and Their Meteorological Controls. Journal of Geophysical Research D: Atmospheres, 2021, 126, e2020JD033459.	1.2	5
110	IASIâ€Derived Sea Surface Temperature Data Set for Climate Studies. Earth and Space Science, 2021, 8, e2020EA001427.	1.1	4
111	Spatio-temporal variations of nitric acid total columns from 9 years of IASI measurements – a driver study. Atmospheric Chemistry and Physics, 2018, 18, 4403-4423.	1.9	3
112	A space view of agricultural and industrial changes during the Syrian civil war. Elementa, 2021, 9, .	1.1	3
113	Transport and Variability of Tropospheric Ozone over Oceania and Southern Pacific during the 2019–20 Australian Bushfires. Remote Sensing, 2021, 13, 3092.	1.8	2
114	Understanding the Simulated Ammonia Increasing Trend from 2008 to 2015 over Europe with CHIMERE and Comparison with IASI Observations. Atmosphere, 2022, 13, 1101.	1.0	2
115	Atmospheric Composition Applications with IASI and next-generation hyperspectral infrared sounders (IASI-NG and IRS). , 2021, , .		1